Triazinylaniline derivatives as fluorescence probes. Part 4.[1-3] Kinetics and selectivity in the reactions of *N,N*-diethyl-4-(dichloro-1,3,5-triazinyl)aniline with amines, amino acids and proteins relevant to fluorescence labelling

David J. Cowley *

Department of Applied Physical Sciences, The University of Ulster, Coleraine, Northern Ireland, UK BT52 1SA

The kinetics of reaction of the reactive triazinyl dye, *N,N*-diethyl-4-(dichloro-1,3,5-triazinyl)aniline with primary and secondary amines, amino acids, and the proteins bovine brain calmodulin and bovine serum albumin in aqueous media, as monitored by UV–VIS absorption spectroscopy, are reported. In general the reaction is first-order in the dye and in the substrate. Secondary aliphatic amines are more reactive than primary aliphatic amines, and a retarding influence of geminal hydroxy substituents is observed in many cases. The intrinsic reactivity of the dye towards the side chain ε-amino group of lysine is 10 times higher than that for a free *N*-terminal amino group. The influences of pH and temperature on reaction rates have been determined. Selectivity in reaction of the dye ($TACl_2$) with lysine residues of calmodulin and bovine serum albumin, of 1:1 and ≈2:1 dye–protein stoichiometry, respectively, is ascribed to the dominant role played by hydrophobic interactions of dye and protein surfaces. On the basis of the kinetic evidence a three-stage mechanism is proposed and numerically evaluated. Initial rapid diffusional encounter of the dye and protein is followed by a slower 'internalization' of the dye in a hydrophobic pocket of the protein (activation energy 65–77 kJ mol^{-1}). Finally, chemical adduct formation occurs in the protein interior having an activation energy of 21–36 kJ mol^{-1}, significantly lower than that found (42–48 kJ mol^{-1}) for reaction of dye and primary aliphatic amines in homogeneous solution.

Introduction

The labelling of particular components with extrinsic fluorescent probes allows selective examination of molecular behaviour in a complex biomolecular assembly, such as that of large complex protein aggregates or of peptides in lipid membranes, *via* the observed optical characteristics of the probes or alterations in such properties caused by environmental or conformational changes in the biomolecules. However, efficient and site-selective introduction of a fluorescent probe entity into a biomolecule is not a trivial problem in many cases.[4-6] In general, coupling reactions need to be performed in a highly aqueous environment not too far removed from physiological conditions of pH, temperature and ionic strength to avoid irreversible denaturation or destruction of the protein or other biosystem. For most biomolecules as substrates in aqueous solution, thiols and amines are the only two groups that can be reliably modified;[6] carboxylic acids and alcohols, including phenols such as tyrosine, are abundant in proteins, *etc.*, but their reactivity in aqueous solutions is low.

Several alkylating reagents R–X exist to modify thiol groups –SH with high chemical selectivity, where the leaving group X may be Cl, Br, I, a sulfonate ester, or part of an aziridine ring. The resultant product –S–R is less stable when X involves an isothiocyanate or succinimidyl ester moiety, which are often used to label reactive amine groups. The latter groups, as a free *N*-terminus or in ubiquitous lysine residues in proteins, react with many reagents in a nucleophilic displacement reaction at a rate dependent on the class of amine and its basicity (and thus also on the pH of the aqueous solution phase which controls the concentration of the free base form). In terms of efficiency of labelling reagent usage, and also the ease of purification of labelled substrate, pH-dependent hydrolysis or other degradation of the labelling reagent must always be taken into account.[4,6]

In addition to the chemical and steric factors operative in such coupling reactions occurring in homogeneous solution, the existence of conformational constraints, local hydrophobic and other, *e.g.*, hydrogen bonding interactions between the labelling reagent and the biomolecule, can serve to modulate greatly the reactivity of a given site in the latter and thus profoundly affect the regioselectivity of the fluorescent labelling process.

Comparative results on the reaction kinetics and site selectivity for reactions of the triazinylaniline chloride dye, *N,N*-diethyl-4-(dichloro-1,3,5-triazinyl)aniline, $TACl_2$, with simple and hydroxy-substituted aliphatic amines, amino acids, neuropeptide Y, calmodulin, and bovine serum albumin are presented which demonstrate the important features in selective labelling and allow assessment to be made of the controllable parameters open to the experimenter to enhance the chances of success in site-selective labelling. The reactive dye, $TACl_2$, has been used to prepare fluorescent membrane probes[2] and to label bovine brain calmodulin at lysine-75 for steady-state and time-resolved fluorescence studies[3] reported previously.

Experimental

Materials

The reactive dye *N,N*-diethyl-4-(dichloro-1,3,5-triazinyl)aniline was prepared and purified as described previously.[1,3]

The amines *n*-butylamine, *n*-hexylamine, *N*-methyl-*n*-butylamine, 2-aminoethanol (ethanolamine), 3-amino-propane-1,2-diol, 2-amino-2-methylpropan-1-ol, 2-(ethylamino)ethanol, ethylenediamine, diaminohexane-1,6-diamine, and piperidine were obtained from Aldrich as general purpose reagents and were used as received. Tris(hydroxymethyl)aminomethane as its hydrochloride salt and the amino acids L-alanine, L-leucine, L-cysteine, L-glutamine and L-proline were used as received from

Sigma as were the hydrochloride salts of L-lysine, L-arginine, L-histidine, and (+)-epinephrine and the sodium salt of L-tyrosine.

Bovine serum albumin (BSA, fraction V, fatty acid free) was obtained also from Sigma and used without further purification. Calmodulin (CaM) was isolated from bovine brain and purified as described elsewhere.[7] Porcine neuropeptide Y (NPY) was synthesized by standard solid-phase peptide synthetic methods using BOC/Bzl chemistry, purified by gel filtration (G10 Sephadex) and preparative C_{18} reversed-phase HPLC, and identity and purity confirmed by amino acid analysis and FAB-MS, by Saudek and Pelton as reported by them previously.[8]

Acetonitrile used in all the kinetic investigations was UVASOL grade from Merck.

Methods

(*a*) Reaction kinetics in homogenous solution. Reaction between the reactive labelling reagent $TACl_2$ and the amines, *etc.* was typically conducted at 298.2 K in 50% v/v aqueous acetonitrile, prepared from stock aqueous solutions of the amines, or buffered amino acid stock solutions, and acetonitrile, and monitored by continuous UV–VIS absorption measurements using a Perkin-Elmer Lambda 5 spectrophotometer, after addition and rapid mixing of a concentrated stock solution of $TACl_2$ in acetonitrile (30 mm^3, *ca.* 2 mmol dm^{-3}) to 3 cm^3 of the reaction mixture in a thermostatted 10 mm path length quartz cuvette. The initial dye reagent exhibits an absorption maximum at 405 nm and the reaction products from saturated amines and amino acids show an absorption maximum at *ca.* 375 nm; an isosbestic point was observed at *ca.* 386 nm indicative of a simple overall conversion A ⟶ B. The decrease in absorbance at 405 nm with time was normally chosen for analysis of the reaction kinetics. In all kinetics experiments the amine or other reactive substrate concentration [S] was at least 100 times greater than that of the dye, and thus the decay of the absorbance D with time t followed strictly pseudo-first-order kinetics. Data points were fitted by least-squares analysis to a function of the form of eqn. (1), from

$$\log \{D(t) - D(\infty)\} = -k_1 t + \text{constant} \qquad (1)$$

which k_1 was obtained and thence the second-order rate constant $k_2 = k_1/[S]$.

(*b*) Fluorescent labelling of neuropeptide Y. Neuropeptide Y was labelled almost exclusively at its *N*-terminal amino group on reaction with the reactive dye $TACl_2$ by nucleophilic substitution of one chlorine atom [1,9,10] under the following conditions.

Neuropeptide Y (3.6 mg) was dissolved in 200 mm^3 MeCN and 400 mm^3 aqueous Tris buffer (100 mmol dm^{-3}, pH 8.3) and 600 mm^3 of the dye $TACl_2$ in MeCN (2 mmol dm^{-3}) added. Reaction at 313 K over several hours was monitored by HPLC analysis and also, after dilution of 30 mm^3 aliquots into 3 cm^3 aqueous MeCN, by UV spectroscopy—since the dye absorbs maximally at 405 nm and the coupled product at 375 nm. Use of a large excess of dye over NPY with extended reaction times led to the appearance of many labelled products subsequent to the initial major adduct. The major fluorescent adduct TANPY was readily separated from unchanged NPY and $TACl_2$, hydrolysed dye, and minor labelled products by C_4 reversed-phase HPLC using aqueous acetonitrile [containing 0.1% trifluoroacetic acid (TFA)] gradient elution (initially 28% v/v acetonitrile, rising linearly to 47% over 30 min at 1.5 ml min^{-1} flow rate; retention times at 16.8 and 21.1 min for NPY and TANPY, respectively).

Electrospray-MS analysis showed a clean spectrum showing the 4, 5 and 6+ ions, mean MH^+ 4515.32 (calc. = 4514.68), of the 1 : 1 dye-NPY adduct.

The intensity ratio of the 277 nm band to the 375 nm band in the UV–VIS absorption spectrum was also as expected for a 1 : 1 TANPY adduct.

The TA label location was deduced from microsequencing experiments on TANPY and peptides isolated by C_4 reversed-phase HPLC from tryptic digests of NPY and TANPY. Attempted microsequencing of TANPY failed to yield any significant amounts of amino acids on the first and subsequent steps whereas NPY yielded the correct amounts of tyrosine, proline, serine, *etc.* under identical conditions, indicating a blocked *N*-terminus in TANPY.

Trypsin digestion of TANPY and NPY (5% trypsin, 50 mmol dm^{-3} Tris buffer at pH 8, 310 K, 4 h, quenching with 1% TFA) followed by HPLC analysis revealed a peptide A at 10.79 min derived from NPY and absent in the TANPY digest, and conversely a peptide B at 18.50 min derived from TANPY and absent in the NPY digest, with all other peptide fragments in common.

Microsequencing of peptide A gave the expected order of amino acids for the *N*-terminal sequence of NPY (residues 1–9 measured) but signalled a failure of NPY to cleave at lysine-4. Peptide A is presumed to consist of residues Tyr1–Arg19 of NPY. The complementary peptide B derived fromTANPY, like the parent TANPY, failed to generate amino acids above background impurities on attempted microsequencing. Thus the structure of TANPY, using conventional letters for the amino acid residues, is (TACl)NH-YPSKPDNPGEDAPAEDLARYY-SALRHYINLITRQRY-NH_2.

The mono-labelled product is formed selectively below pH 9. Displacement of the remaining chlorine on the triazine ring in the labelled peptide occurs very slowly (*ca.* 10% reaction over 5 days at 293 K in aqueous solutions at neutral pH), due to the much reduced electrophilicity of the triazine ring in TANPY compared with that in the parent $TACl_2$ dye (Shaw and Ward, 1973).

(*c*) Fluorescent labelling of bovine brain calmodulin. To 1 cm^3 of a buffered aqueous stock solution of calmodulin (100–150 μmol dm^{-3} CaM, 50 mmol dm^{-3} Tris at pH 7.0–8.7) containing calcium ion (0–4 mmol dm^{-3}) was added 5 mm^{-3} of a near-saturated solution of $TACl_2$ in acetonitrile (*ca.* 2 mmol dm^{-3}). The reaction was monitored by the decay in absorbance at 405 nm.

(*d*) Reaction kinetics and fluorescent labelling of bovine serum albumin. (*i*) *Reaction kinetics.*—To 3 cm^3 of a buffered aqueous stock solution of bovine serum albumin (typically 2 mg ml^{-1} BSA, 100 mmol dm^{-3} Tris at pH 8.0, ±100 mmol dm^{-3} KCl) were added 15 mm^{-3} of a near-saturated solution of $TACl_2$ in acetonitrile (*ca.* 2 mmol dm^{-3}). The reaction was monitored by the decay in absorbance at 405 nm with time; the kinetic rate constants were evaluated using the expression given in Methods section (*a*) above, and as discussed in the Results. In some experiments repetitive scans of the absorption spectrum in the wavelength range 340–460 nm were made which revealed a shift of the isosbestic point under certain conditions.

(*ii*) *Stoichiometry of reaction.*—To 1 cm^3 aliquots of a 50 μmol dm^{-3} solution of BSA (50 mmol dm^{-3} Tris buffer containing 0.15 mol dm^{-3} NaCl, pH 8.0) were added known aliquots (0, 10, 20, ... 100 mm^{-3}) of a 2.016 mmol dm^{-3} solution of $TACl_2$ in acetonitrile. After 30 min reaction at 298 K each sample was centrifuged and the UV–VIS absorption spectrum of the supernatant recorded, followed by addition of 1.5 cm^3 buffer (50 mmol dm^{-3} Tris buffer containing 0.15 mol dm^{-3} NaCl, pH 8.0). The 2.5 cm^3 of sample was loaded onto a short-form Sephadex G25 column and eluted with 3.5 cm^3 of the buffer. The UV–VIS absorption spectrum of the eluate was recorded. The contribution of the TA chromophore to the absorbance at 280 nm of the BSA–TA adduct was subtracted from the observed absorbance of the BSA–TA adduct at 280 nm wavelength. This contribution was estimated to be 6.9% of the absorbance at the TA chromophoric band maximum at 375 nm in the amine adduct, on the basis of the UV absorption spectrum of the 1 : 1 adduct of $TACl_2$ with butylamine. The

Table 1 Reaction of $TACl_2$ with amines and hydroxide ion: variation of first-order rate constant k_1 with concentration of nucleophile [a]

[Butylamine]/mmol dm^{-3}	$k_1/10^{-3}$ s^{-1}	[Piperidine]/mmol dm^{-3}	$k_1/10^{-3}$ s^{-1}	[Hydroxide]/mmol dm^{-3}	$k_1/10^{-3}$ s^{-1}
0.80	1.61	0.32	17.7	3.98	2.20
1.60	3.32	0.64	45.9	5.96	3.07
3.20	6.90	0.96	70.4	11.9	5.29
4.79	10.45	1.28	90.0	29.1	10.7
				45.8	16.3
				63.7	21.3
				91.0	30.8

[a] Solvent: 50% v/v MeCN–water at 298.2 K. Initial concentration of $TACl_2 \approx 0.03$ mmol dm^{-3} ≪ [nucleophile], and thus the kinetic rate law is of the form $-d[TACl_2]/dt = k_1[TACl_2]$.

ratio of the absorbance at 375 nm (UV absorption maxima of the BSA–TA adduct) to the corrected absorbance at 280 nm as a function of the original addition of $TACl_2$ showed a distinct break point. The slope of the plot up to that point allowed estimation of the molar extinction coefficient of absorption of the TA chromophore in the BSA–TA adduct. Both the limiting value of the absorbance ratio and the break point concentration of added $TACl_2$ dye allowed the stoichiometry of the adduct to be calculated independently as described in the Results.

Results and discussion

(*f*) Reaction of $TACl_2$ with primary and secondary aliphatic amines in homogeneous solution

The reactive triazinyl dichloride dye, $TACl_2$, readily couples to primary and secondary aliphatic amines at room temperature in aqueous acetonitrile, and in most organic solvents, *e.g.*, from diethyl ether to dimethylformamide, with displacement of one chloride anion.[11,12] (Facile reactions also occur with several tertiary aliphatic amines, pyridines and imidazoles which are not reported here, since there are obvious mechanistic differences and the results are not relevant to labelling of proteins by the reactive dye.)

Mono-replacement of chlorine is revealed by the intense UV absorption band maximum of the $TACl_2$–amine adduct at *ca.* 370 nm. The second chlorine of the dye moiety may be replaced only under more forcing conditions of elevated temperature (>330 K) and/or high concentrations of the more reactive secondary aliphatic amines.[1,2] The product of such disubstitution of chlorine for amino groups possesses an intense UV absorption band maximum at *ca.* 345 nm. The existence of a clean isosbestic point (382–387 nm) and product absorption at 365–370 nm reveals the simple mono-substitution nature of the reactions occurring under the mild conditions examined in this study. Secondary aliphatic amines were examined only at low concentrations (<mmol dm^{-3}) and in all substrates the concentration ranges were selected to provide reaction half-lives around 5–10 min and always >30 s.

(*a*) Order of reaction w.r.t. $TACl_2$. In the presence of an excess concentration of amine substrate the decay of the reactant dye concentration, monitored by the decrease in UV absorbance A_t at 405–410 nm with time t, was mono-exponential to a small final value A_∞. Plots of $\log(A_t - A_\infty)$ *versus* time were strictly linear, with correlation coefficients R better than 0.998 in all cases, indicating that the reaction is first-order in the concentration of the TA dye reactant.

(*b*) Order of reaction w.r.t. amine nucleophile. The first-order rate constants k_1 were measured for the decay of the dye reactant as a function of the concentration of the various amines, with the latter being in great excess (normally >100 fold) over the former. Typical results are given in Table 1. The linear variation of k_1 with nucleophilic concentration shows that the coupling reaction is also first-order in the concentration of the amine or other nucleophile under the conditions.

Table 2 Reaction of $TACl_2$ with amines: second-order kinetic rate constant k_2 and nucleophile chemical structure

Nucleophile	k_2/dm^3 mol^{-1} s^{-1}
Butylamine	2.11 ± 0.06
Hexylamine	0.52 ± 0.04
Ethane-1,2-diamine	0.95 ± 0.08 [a]
Hexane-1,6-diamine	3.02 ± 0.20 [a]
2-(Ethylamino)ethanol	1.50 ± 0.08
N-Methylbutylamine	26.0 ± 1.0
Piperidine	72.0 ± 2.0
(±)-Epinephrine [4-(1-hydroxy-2-methylaminoethyl)benzene-1,2-diol]	23.0 ± 2.5 [a]
Ethanolamine	0.027 ± 0.005
3-Aminopropane-1,2-diol	0.35 ± 0.03
2-Amino-2-methylpropan-1-ol	0.0073 ± 0.002
Hydroxide ion	0.33 ± 0.015

[a] Solvent: 50% v/v MeCN–Tris buffer, pH 11, at 298.2 K. Solvent in all other cases, 50% v/v MeCN–water, at 298.2 K.

Reaction: $TACl_2 + R^1R^2NH \longrightarrow TA(Cl)NR^1R^2 + (HCl)$

Initial concentration of $TACl_2 \approx 0.03$ mmol dm^{-3} ≪ [nucleophile], and thus the kinetic rate law is of the form $-d[TACl_2]/dt = k_2$ [nucleophile] $[TACl_2] \Rightarrow k_1[TACl_2]$.

(*c*) Overall rate law. The full rate expression is given in eqn. (2). The second-order rate constants were derived thus by

$$-d[TACl_2]/dt = k_2[TACl_2][\text{amine}] = k_1[TACl_2] \quad (2)$$

the relation $k_2 = k_1/[\text{amine}]$. Table 2 gives the values of k_2 so obtained for a representative series of aliphatic amines. Mechanistic aspects of similar (pseudo-aromatic) nucleophilic substitutions involving azines have been well characterized.[11–19]

(*d*) Relationship between second-order rate constants and the chemical structure of the amine. As expected the secondary amines, being more basic, are more than an order of magnitude more reactive than related primary amines, *e.g.*, *N*-methylbutylamine and butylamine, with piperidine being significantly a very effective nucleophile. The length of the alkyl chain, and its distant substitution, in the primary aliphatic amines does not introduce any major perturbation to the reactivity, *e.g.*, compare k_2 (butylamine) = 2.11 dm^3 mol^{-1} s^{-1}, $\frac{1}{2}k_2$ (hexane-1,6-diamine) = 1.51 dm^3 mol^{-1} s^{-1}, and k_2 [2-(ethylamino)ethanol] = 1.50 dm^3 mol^{-1} s^{-1}. The presence of an hydroxysubstituent *geminal* to the primary amine group may cause a substantial reduction in reactivity attributable to internal hydrogen bonding involving the lone pair electrons of the amino nitrogen centre. The effect is most noticeable in the cases of ethanolamine and 2-amino-2-methylpropan-1-ol (see Table 2), and also for the buffer Tris for which $k_2 < 0.003$ dm^3 mol^{-1} s^{-1} at pH 11.0 was estimated. Tris buffer is thus preferred for protein labelling experiments using the dye $TACl_2$, over buffers such as MES and PIPES since the latter contain secondary amino groups and react efficiently with the dye at pH > 8. Exceptionally, the presence of two hydroxy groups mutually adjacent reduces the retardation imposed on the primary amine

Table 3 Second-order kinetic rate constant k_2 for the reaction of $TACl_2$ with butylamine at 298.2 K in binary mixtures of acetonitrile and water[a]

% v/v Water in acetonitrile	k_2/dm^3 mol^{-1} s^{-1}
65.7	2.98
49.5	2.18
33.5	1.64
17.6	1.55
9.58	1.76
4.79	2.36
1.60	3.22
0.0	4.73

[a] In neat butyronitrile and in neat tetrahydrofuran k_2 was 3.91 and 4.53 dm^3 mol^{-1} s^{-1}, respectively. Initial concentration of $TACl_2 \approx 0.03$ mmol dm^{-3} $\ll$ [*n*-butylamine] = 4.8 mmol dm^{-3}.

Table 4 Second-order kinetic rate constant k_2 for the reaction of $TACl_2$ with amino acids in 50% v/v aqueous acetonitrile at 298.2 K

	Rate constant k_2/dm^3 mol^{-1} s^{-1}				
...no acid	*N*-Terminal amino		Side chain nucleophilic group		Apparent pK_a
L-Alanine	0.108	*a*			
L-Leucine	0.203	*a*			
L-Glutamine	0.066	*a*			
L-Proline	55.0	*b*			11.2 (α-NH)
L-Arginine	0.30	*c*			9.3 (α-NH_2)
L-Histidine	0.130	*d*	(0)		9.80 (α-NH_2)
L-Tyrosine	<0.17	*f*	3.7	*e*	*ca.* 11 (ArOH)
L-Lysine	0.10	*f*	1.08	*g*	10.8 (ε-NH_2)

[a] Estimated from k_2 value at pH 11.0. [b] Estimated from k_2 value at pH 12.7. [c] Estimated from k_2 value at pH 12.0. [d] Estimated from k_2 value at pH 12.3. [e] Estimated from k_2 value at pH 11.6. [f] Estimated from k_2 value at pH < 9.0. [g] Estimated from k_2 values at pH > 12.0. Solvent: 50% v/v MeCN–water at 298.2 K. Initial concentration of $TACl_2 \approx 0.03$ mmol dm^{-3} $\ll$ [amino acid], and thus the kinetic rate law is of the form $-d[TACl_2]/dt = k_2[\text{amino acid}][TACl_2] \Rightarrow k_1[TACl_2]$.

reactive centre in 3-aminopropane-1,2-diol, perhaps by preferential mutual hydrogen bonding of the hydroxy groups. Hydroxide ion is seen to be a poorer nucleophile intrinsically than an aliphatic primary amine.[18]

***(e)* Effects of solvent composition.** The role of solvent,[19] in terms of polarity and propensity towards hydrogen bonding, was not investigated comprehensively. Results for the butylamine–$TACl_2$ reaction in binary mixtures of water and acetonitrile are given in Table 3. The variation in second-order rate constant with solvent composition is not pronounced and no great advantage in reaction rate is to be gained by judicious choice of aqueous solvent media.

(II) Reaction of $TACl_2$ with amino acids in homogeneous aqueous solution

Kinetic studies on the reaction of $TACl_2$ with amino acids were performed analogously to those with the aliphatic amines using aqueous solutions whose pH was controlled by addition of Tris buffer. The apparent second-order rate constants were evaluated likewise from measurements of the apparent first-order rate constants at various excess concentrations of the amino acid (Table 4).

***(a)* Effects of pH on apparent rate constants.** Since only the free base form of the ionisable amino acids acted as nucleophile in displacement of chlorine from the triazinyl chloride dye a sigmoidal dependence of the rate constant on pH of the solution was observed, as shown for example in Fig. 1 for lysine and histidine where the observed first-order rate constant normalized to the maximum value attained at very high pH is plotted against pH. The mid-point allows estimation of the apparent pK_a for the conjugate acid of the reactive amine group (Table 4). In the cases of lysine and tyrosine the contributions to the

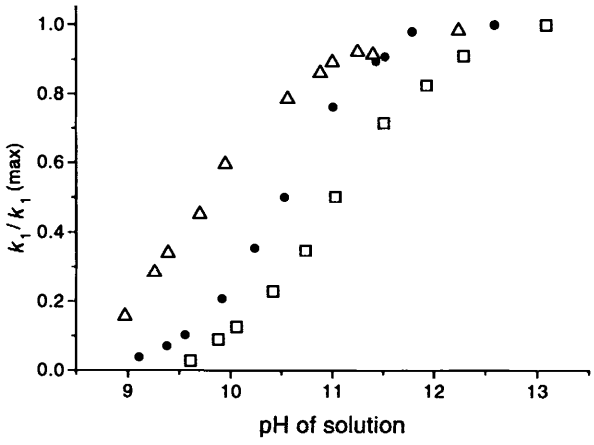

Fig. 1 Variation of the relative first-order rate constant k_1 for reaction of $TACl_2$ with lysine (□) and histidine (△) with pH. ● show the expected curve for a reactant system having pK_a = 10.5. Solvent 50% v/v MeCN–50% Tris buffer (0.1 mol dm^{-3}) at 298 K. Initial concentrations of lysine and histidine were 11 and 100 mmol dm^{-3}, respectively.

rate constant by the α-amino group are close to the values obtained for the neutral amino acids such as alanine or leucine, and were estimated from the low reaction rates at pH < 9, where the contributions from the ε-amino group and the phenoxy group of the side-chains, respectively, are negligible. Above pH 9.5 coupling to the triazine ring of the dye by the phenoxy group of tyrosine is demonstrated by the large red shifts in both the product UV absorption maxima and the isosbestic point to 388 and 394 nm, respectively, by comparison with those for coupling to saturated amines.

***(b)* Side-chain and *N*-terminal amino group reactivities.** The intrinsic reactivity towards $TACl_2$ of a free α-amino group (k_2 values 0.07–0.2 dm^3 mol^{-1} s^{-1}) in the amino acids is 10 times lower than that of a primary amine group in aliphatic amines (compare Tables 2 and 4) owing to the proximity of the carboxylate group and its inductive effect on the α carbon atom. The intrinsic reactivity of the free ε-amino group of lysine (k_2 = 1.08 dm^3 mol^{-1} s^{-1}) is close to that of the primary amine group in butylamine (k_2 = 2.11 dm^3 mol^{-1} s^{-1}) and hexylamine (k_2 = 0.52 dm^3 mol^{-1} s^{-1}) as expected. The phenoxide moiety of tyrosine is a somewhat better nucleophile[6]—attributable in part to the expected partial conjugative stabilization of the transition state in this case. The guanidinium base of the arginine side-chain appears to be unreactive towards $TACl_2$.

(III) Potential control of relative reactivity in the reaction of $TACl_2$ with amino groups

Parameters that are both relevant to the site selectivity of the labelling reaction and also open to the control of the experimenter are limited. They include the solution pH, temperature, and serendipitous or engineered utilization of hydrophobic interactions between the reactive dye and the protein. Such possibilities are now examined by reference to the reactions of $TACl_2$ with NPY, CaM and BSA.

***(a)* Manipulation of pH.** Use of mildly alkaline solution, *e.g.*, at pH 8, can favour reaction of an α-amino group at a protein/peptide *N*-terminus (p$K_a \approx 9.0$) over reaction at an ε-amino group of lysine since the free base form of the latter (p$K_a \approx 10.5$) may be less than 3% of the free base form of the former and offset, with respect to relative reaction rates, the ten-fold greater intrinsic reactivity.[6] Thus, as described in the Experimental section, labelling of porcine NPY with $TACl_2$ at pH 8.3 led cleanly to the *N*-terminally labelled adduct (>90% of all labelled products) and not at residue lysine-4. Prolonged reaction times with a >five-fold molar excess of dye over peptide, or use of higher pH, *e.g.* pH 10, led to complex mixtures of

Table 5 Arrhenius activation energies for reaction of $TACl_2$ with amines and amino acids[a]

Compound	E_a/kJ mol^{-1}	Conditions
Butylamine	43.1 ± 1.2	
Hexylamine	41.9 ± 1.5	
L-Lysine	48.5 ± 1.0	pH 12.05
L-Histidine	59.2 ± 1.1	pH 9.3 and 10.9
L-Tyrosine	51.2 ± 3.3	pH 11.0
N-Methylbutylamine	32.4 ± 1.1	
Piperidine	27.0 ± 1.0	

[a] All reactions with the amines were performed using 50% v/v aqueous acetonitrile as solvent, and in 50% v/v aqueous Tris buffer (0.1 mol dm^{-3})–acetonitrile for the amino acids.

products which may have included dye adducts at tyrosines 1, 20, 21, 27 and 36. Analogous behaviour has been reported for the reaction of melittin with 1-fluoro-2,4-dinitrobenzene.[20]

***(b)* Selection of temperature.** The influence of temperature on the rates of the $TACl_2$–amine/amino acid coupling reactions was investigated. Table 5 collates activation energies derived from Arrhenius plots of log (apparent first-order rate constant) *versus* inverse temperature. The activation energy for the nucleophilic displacement reaction of chloride ion from the triazinyl chloride is significantly lower for the secondary than for the primary aliphatic amines. Reaction of an α-amino group, *e.g.*, in histidine, has a higher activation energy than reaction at a lysine ε-amino group (difference ≈ 10–15 kJ mol^{-1}, corresponding to a 1.50–1.84-fold rate *differential* for change of temperature from 283 to 313 K). Thus reaction at an *N*-terminal amino group may be favoured marginally by choice of a higher temperature for the labelling reaction consistent with the stability of the protein.

***(c)* Utility of hydrophobic and other dye–protein interactions.** Specific molecular interactions[21–23] between the reactive triazine dye label and specific residues of a water soluble protein, utilizable in affinity chromatography,[21] as well as general solubilization of a poorly water-soluble dye in hydrophobic pockets of a protein, may result in a strong restriction on the promiscuity of the dye–reactive amino acid residue coupling. This may arise by a combination of accessibility and orientational restriction for approach to the reaction transition state and by microenvironmental effects which provoke differences in the intrinsic reactivities of potential reactive groups. Effective protonation affinities (as deduced by apparent pK_a values) are known to range widely depending on detailed interactions in the protein interior.[24] The interplay of these factors, alongside those previously examined, is now considered with reference to experimental studies of fluorescence labelling of calmodulin and bovine serum albumin by $TACl_2$.

(*IV*) Reaction of $TACl_2$ with calmodulin

At high (>3 mmol dm^{-3}) concentrations of calcium ion, bovine brain calmodulin has been shown to react with $TACl_2$ almost exclusively[25,26] at lysine-75, near to the 'expansion joint'[27–29] of the central α-helical region of this important protein.[30–34] Outline studies of the kinetics reveal a pH dependence of the reaction rate compatible with reaction at lysine (Table 6). The experimentally accessible pH range was limited to <pH 9 by protein stability and did not permit determination of the effective pK_a of the reactive residue.

The concentration of calcium ion plays a major role in determining both the reaction rate and the efficiency of labelling (Table 7). Binding of calcium[35,36] at the four specific capital sites, two of higher affinity (sub-micromolar) in the *C*-terminal domain consisting of two EF hands and two of weaker affinity (micromolar) in the corresponding *N*-terminal domain,[37] exposes hydrophobic patches on the protein inaccessible in apocalmodulin to which target peptides/proteins may bind. Auxillary binding of calcium, and other divalent cations, occurs at

Table 6 Dependence on pH of the first-order rate constant k_f for reaction of $TACl_2$ with bovine brain calmodulin at high concentration of calcium ion[a]

Solution pH	$k_f/10^{-3}$ s^{-1}
7.00	0.30 ± 0.03
7.64	0.42 ± 0.04
8.00	1.12 ± 0.02
8.20	1.09 ± 0.02
8.40	1.93 ± 0.05
8.54	2.28 ± 0.03
8.73	2.51 ± 0.02

[a] Reaction at 295 K in Tris buffer (100 mmol dm^{-3}). Concentration of calcium ion 1.86 mmol dm^{-3}. Initial concentrations of calmodulin and dye reagent $TACl_2$ were 137 and 15 μmol dm^{-3}, respectively. The apparent first-order rate constant k_f is defined by the equation, $-d[TACl_2]/dt = k_2[TACl_2][calmodulin] = k_f[TACl_2]$, since under the conditions [calmodulin] is nearly constant.

Table 7 Dependence of the rate of reaction of $TACl_2$ with bovine brain calmodulin at pH 8.4 on the concentration of calcium ion[a]

[Calcium ion]/ mmol dm^{-3}	R (init)[b]	Final product absorbance at 370 nm[c]	$k_f/10^{-3}$ s^{-1}[d]
0	1.46	0.15	?
0.24	1.67	0.18	?
0.48	3.17	0.30	1.12
1.87	7.13	0.62	1.94
3.56	7.40	0.62	2.03

[a] Reaction at 295 K in Tris buffer (100 mmol dm^{-3}); initial concentrations of calmodulin and dye reagent $TACl_2$ were 137 and 15 μmol dm^{-3}, respectively. [b] Relative initial rate R(init) = 10^4 (decrease in absorbance at 405 nm s^{-1}) for the time period 0–180 s. [c] The absorbance due to the dye–calmodulin adduct shows a maximum at 370 nm under these conditions. The initial absorbance due to the dye reagent at 405 nm was 0.68 ± 0.02 in each case. [d] Apparent first-order rate constants k_f were evaluated only for those cases for which good linear plots of log(A_{405}) *versus* time were obtained.

millimolar concentrations of such ions[3,35] which leads to further exposure of, and alterations to, certain hydrophobic surfaces by sliding adjustments of α-helices. These conformational transformations have been the subject of many studies by NMR, X-ray crystallographic and spectroscopic methods.[29–33] Binding of calcium ions has also been shown to modulate dramatically the reactivities of the lysine residues in calmodulin towards electrophilic reagents.[38–43]

Studies by us on the steady-state and time-resolved fluorescence properties of calmodulin labelled at lysine-75 with $TACl_2$ (TACaM) show that the triazinylaniline dye label resides in a highly hydrophobic environment when TACaM has calcium ions bound at both capital and auxillary binding sites.[3] Since the approach to the transition state of the dye–reactive lysine-75 system must involve a protein microenvironment similar to that of the covalently bound probe dye in TACaM, the accelerating effect of calcium loading on the reaction rate is understandable. The reactive dye molecule experiences a strong hydrophobic attraction to a central hydrophobic region of the protein, possibly assisted by hydrogen bonding of the azine nitrogens to H-donor side-chains of serine residues, *etc.*,[22,23] and there encounters a lysine side-chain whose reactivity has been enhanced by the same hydrophobicity of the protein interior in this region. Thus, serendipitously, the site selectivity of fluorescent labelling is high.

The ability, or inability, of a protein to solubilize a reactive hydrophobic dye also has practical consequences, which are demonstrated in the $TACl_2$–calmodulin system. The dye has a low solubility *per se* in aqueous solution (<4 μmol dm^{-3}); addition of a concentrated solution of the dye in acetonitrile to aqueous buffer results in a slow (10 min) precipitation. Dilute solutions of calmodulin (100–200 μmol dm^{-3}) at lower concen-

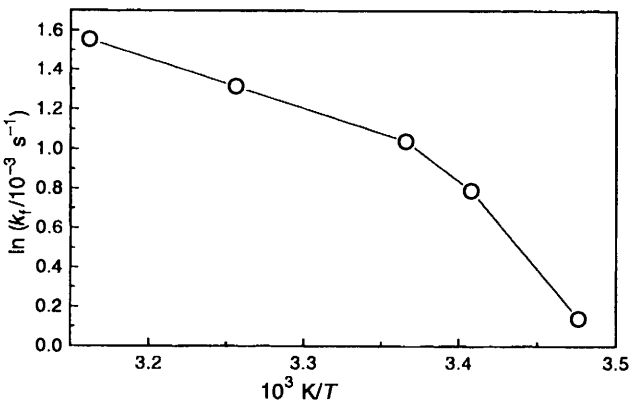

Fig. 2 Arrhenius plot of the first-order rate constant (final limit k_f) for reaction of $TACl_2$ with bovine brain calmodulin in the presence of excess calcium ion (3.56 mmol dm^{-3}) at pH 8.55 (Tris buffer). Initial concentrations of $TACl_2$ and calmodulin were 15 and 120 μmol dm^{-3}, respectively.

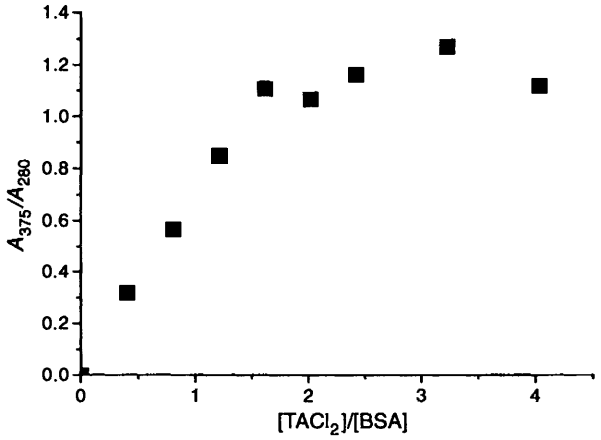

Fig. 3 Variation of the ratio of UV absorptions at 375 nm (due to the TA fluorophore alone) and at 280 nm (due >95% to BSA protein) with the stoichiometric ratio of the reactants $TACl_2$ and BSA in the initial reaction mixture, after gel chromatographic separation of the TA-labelled protein. Reaction performed in Tris buffer (100 mmol dm^{-3}, pH 8.0, 298 K) for 30 min. Initial concentration of BSA was 50 μmol dm^{-3}.

trations of calcium ion upon such addition of $TACl_2$ in acetonitrile become cloudy, since the protein is unable to solubilize the dye completely. Correspondingly, the final yield of labelled TACaM product, as judged by its characteristic UV absorption at 370 nm, is reduced since reaction must compete with precipitation of the dye (see Table 7). At high concentration of calcium ion the calcium-loaded calmodulin can solubilize the dye effectively and the intrinsic rate of the coupling reaction is faster leading to high efficiency of labelling.

The influence of the prior solubilization step on the reaction kinetics is also detectable in the Arrhenius plot (Fig. 2) of the apparent pseudo-first-order rate constant *versus* inverse temperature. At lower temperatures the slope corresponds to an activation energy of 77 kJ mol^{-1} which changes to 21 kJ mol^{-1} above *ca.* 295 K. It is conceivable that a conformational change in the calmodulin could produce such a result. More likely, however, is an explanation involving several kinetic steps of solubilization and reaction, since analogous behaviour was observed with the $TACl_2$–BSA system as reported and analysed below.

(*V*) Reaction of $TACl_2$ with bovine serum albumin

Serum albumin, the major soluble transport protein for unesterified fatty acids in plasma,[44] possesses several binding sites/pockets for a variety of chemically diverse ligands, *e.g.*, fatty acids,[45] porphyrins,[46] pyridoxal 5′-phosphate[47] and L-tryptophan.[48] The principal regions for ligand binding in human serum albumin (M_r 65 kDa) are located in hydrophobic cavities in sub-domains IIA and IIIA. Since the dye $TACl_2$ is hydrophobic in nature and should be solubilized in the readily available BSA, this system was chosen for detailed kinetic study. *A priori*, there are 57 lysine and 19 tyrosine residues at which reaction may occur[49] and hence provide a test of any selectivity imposed by the constraints of hydrophobic interactions between dye and protein. The features of the solubilization kinetics in relation to the chemical coupling reaction(s) are of interest as a guide for the labelling of other proteins.

(*a*) Determination of reaction stoichiometry. Since the possibility of multiple labelling of the protein was high it was important to establish the limits, if any, to the labelling stoichiometry before embarking on kinetic studies. The general procedure is described in the Experimental Methods (*d*) (*ii*). For addition of 10, 20, 30 and 40 mm^3 of $TACl_2$ in acetonitrile (2.016 mmol dm^{-3}) to 1 cm^3 of BSA solution (50 μmol dm^{-3}, pH 8), corresponding to dye/protein molar ratios of 0.403, 0.806, 1.209 and 1.613, respectively, the measured absorbances at 375 nm after 30 min reaction time were 0.147, 0.260, 0.376 and 0.477, respectively, for 2 mm optical path length. A mean molar extinction coefficient ε (TABSA) at 375 nm of 27 000 dm^3 mol^{-1} cm^{-1} was calculated for the labelled adduct. The absorption band position indicates reaction at lysine rather than tyrosine residue(s).

After sample dilution and gel separation of labelled and unlabelled BSA from unchanged dye, *etc.*, the UV absorption spectra were again recorded. The ratio of the absorbances at 375 and 280 nm for each sample (corrected as described in the Experimental Methods) varied with the initial molar ratio of dye to protein as shown in Fig. 3. Two independent estimates can be made of the stoichiometry n (= $TACl_2$/BSA molar ratio) from the data.

(*i*) The plateau value for the 375 nm/280 nm absorbance ratio, for $TACl_2$/BSA molar ratio >1.5, is 1.145 ± 0.057. Assuming the molar extinction coefficient of BSA at 280 nm is 43 400 dm^3 mol^{-1} cm^{-1} then n = 1.145 × 43 400/27 000 = 1.84 ± 0.092.

(*ii*) The intersection of the rising linear part of the plot and the plateau (Fig. 3) occurs at n = 1.69 ± 0.10, in reasonable agreement with the preceding estimate.

Thus, under the experimental conditions, the BSA molecule can react readily with a limit of two molecules of dye, from which it is inferred that two major binding pockets are occupied by two covalently coupled fluorescent dye molecules (as is found for reaction of pyridoxal 5′-phosphate with human serum albumin[47]). The drastic limitation on the selection of reactive residues, despite the theoretically wide choice, is evident. What remains unknown is the selectivity for individual lysine residues lining a given pocket. Extensive enzymic digestion studies and peptide sequencing would be required to define this point.

(*b*) Kinetics of reaction. For concentrations of BSA of 2 mg cm^{-3} or above, repetitive scanning of the UV–VIS absorption spectrum after addition of $TACl_2$ (as a concentrated solution in acetonitrile, *ca.* 2 mmol dm^{-3}) revealed the smooth conversion of the free dye (absorption maximum at 410 nm) into the TABSA adduct (absorption maximum at 370 nm); an isosbestic point was found at 387 nm. When the concentration of BSA was lower than 2 mg cm^{-3} (30 μmol dm^{-3}), for an initial concentration of $TACl_2$ of 15–20 μmol dm^{-3}, this isosbestic point was gained only at a much later stage in the reaction. This phenomenon is attributed to a competition between precipitation of the dye and its solubilization/reaction inside the protein.

The decay in absorbance at 410 nm monitors the disappearance of free and solubilized $TACl_2$ reagent. Typical forms of the logarithmic plots required for pseudo-first-order kinetic analysis of the decays are shown in Fig. 4, where, in this case, the temperature was varied for constant initial concentrations of BSA and dye. Analogous plots were obtained for the

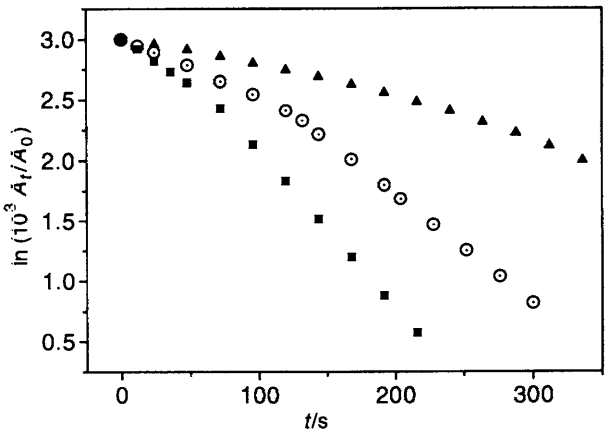

Fig. 4 Apparent first-order kinetic plots for reaction of $TACl_2$ with bovine serum albumin in Tris buffer (100 mmol dm^{-3}, pH 7.95, KCl at 100 mmol dm^{-3}) at 293.3 K (▲), 303.4 K (○) and 313.4 K (■). A_t is the measured UV absorbance at 410 nm at time t. Initial concentrations of $TACl_2$ and BSA were *ca.* 15 and 30 μmol dm^{-3}, respectively.

Table 8 Dependence on protein concentration of the initial rate of reaction of $TACl_2$ with bovine serum albumin in aqueous 0.1 mol dm^{-3} Tris buffer, pH 9.0, at 295 K

[BSA]/mg cm^{-3}	Relative initial rate constant k_1[a]
0.661	0.70
1.32	1.22
2.33	2.19
5.00	5.00

[a] Initial slope of the plot of $\ln(A_t/A_0)$ *versus* time t, relative to that obtained at a BSA concentration of 5 mg cm^{-3} (arbitrarily set to 5.0).

Table 9 Dependence on protein concentration of the final rate of reaction of $TACl_2$ with bovine serum albumin in aqueous 0.1 mol dm^{-3} Tris buffer, pH 9.0, at 295 K

	Limiting first order rate constant $k_F/10^{-2}$ s^{-1}	
[BSA]/mg cm^{-3}	Absence of KCl	KCl (0.1 mol dm^{-3})
1.0	2.73	2.13
2.0	2.83	3.13
3.0	3.00	3.81
4.0	3.30	3.90
5.0	3.30	4.07

The limiting first order rate constant k_f is obtained from the slope of a plot of ln A_{450} (due to $TACl_2$) *versus* time for intermediate and final time periods, *i.e.*, ignoring the initial curvature in the early time period.

variation in the concentration of the BSA protein at constant temperature. Designating the initial and final gradients (pseudo-first-order rate constants) of these plots as k_1 and k_F, corresponding to early and late phases of the reaction, the following empirical observations hold.

(*i*) The initial gradient k_1 increases linearly with increase in [BSA] (see Table 8) and eventually becomes identical with k_F, *i.e.*, at high [BSA] linear plots are found for the whole time course of reaction.

(*ii*) At constant [BSA], increase in temperature increases k_1 which also approaches k_F (Fig. 4).

(*iii*) With increase in [BSA] the final gradient k_F approaches a limit (Table 9) showing only a small dependence on the concentration of added electrolyte KCl.

(*iv*) At constant [BSA] the final gradient k_F (applicable to the majority of the time course, *i.e.*, k_1 equates early to k_F) shows a sigmoidal dependence on the pH of the solution (Fig. 5).. The conjugate acid of the reactive amino group has an apparent pK_a of 9.60 ± 0.15, consistent with that of reactive lysine residues.

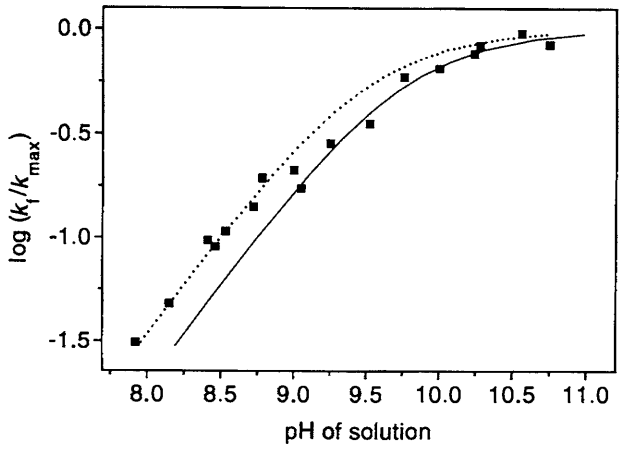

Fig. 5 Variation of $\log(k_f/k_{max})$ with pH of solution for reaction of $TACl_2$ with bovine serum albumin in Tris buffer (100 mmol dm^{-3}, 298 K, KCl at 100 mmol dm^{-3}). The apparent first-order rate constant k_f was determined from the slope of the plot of ln A_{410} *versus* time, at the long time limit if necessary. The maximum value of k_f at high pH = k_{max} = 0.186 s^{-1}. The dotted and solid curves show the expected curves for reactive protein residues having pK_a values of 9.45 and 9.70, respectively.

(*c*) Method of analysis of the kinetic data. Consideration of the data curves and of the likely mechanistic steps indicated analysis by a kinetic scheme involving consecutive pseudo-first-order processes,[50] designated here T ⟶ C (rate constant k_{TC}) and C ⟶ P (rate constant k_{CP}), where T is the free dye, C an intermediate complex of dye solubilized in the protein, and P is the final chemical adduct of dye and protein. One notes, however, that analysis of curved pseudo-first-order plots is not without some danger in that they may arise from mechanisms more complex than the simplest case considered here.

$$\alpha = [T]/[T]_0;\ \beta = [C]/[T]_0;\ \gamma = [P]/[T]_0;\ z = k_{CP}t;\quad x = k_{TC}/k_{CP} \quad (3)$$

Using the normalizing expression[50] (3), where [ ] refers to concentration and subscript zero to time $t = 0$, the integrated expressions for the variation with time of the concentrations of T and C are given in eqn. (4). (This convention was chosen in

$$\alpha = \exp(-zx) \text{ and } \beta = x\{\exp(-zx) - \exp(-z)\}/(1 - x) \quad (4)$$

order to give a time base scaled to k_{CP} since the latter can be estimated directly and unambiguously from the kinetic data at the later times.) If A_t is the absorbance at time t, and if the molar extinction coefficients of T and C are designated ε(T) and ε(C) at the observation wavelength, then eqn. (5) holds.

$$A_t/A_0 = \alpha + \beta\{\varepsilon(C)/\varepsilon(T)\} \quad (5)$$

For the dye $TACl_2$ a good approximation is that $\varepsilon(C) \approx \varepsilon(T)$; eqn. (6) results.

$$y = A_t/A_0 = \exp(-zx) + x[\exp(-zx) - \exp(-z)]/(1 - x) = F(x,z) \quad (6)$$

Plots of $\ln(A_t/A_0)$ *versus* time, obtained from the experimental data, are mimicked well by the family of curves generated for ln $F(x,z)$ *versus* scaled time z using appropriate assumed values of the rate constant ratio 'x'. To evaluate readily the value of x for a given experimental data set recourse was made to the following device. In theoretical, simulated curves the value of z at which $\ln(\alpha + \beta)$ attains a given value, −1 for example, denoted $z[-1]$, correlates smoothly with x thus:

$z[-1]$	1.11	1.28	1.59	1.84	2.05	2.42
x	10	4	2	1.40	1.10	0.80

Table 10 Dependence on temperature of the initial (k_I) and final (k_F) rate constants of reaction of $TACl_2$ with bovine serum albumin[a]

T/K	$k_I/10^{-3}$ s^{-1}	$k_F/10^{-3}$ s^{-1}
323.9	104	22.5
318.8	60.2	17.7
313.6	44.8	12.8
308.5	20.2	11.2
303.4	20.7	9.1
298.4	11.0	7.3
293.3	8.3	5.2

[a] [BSA] = 2 mg cm^{-3} in 0.1 mol dm^{-3} Tris buffer, pH 8.0.

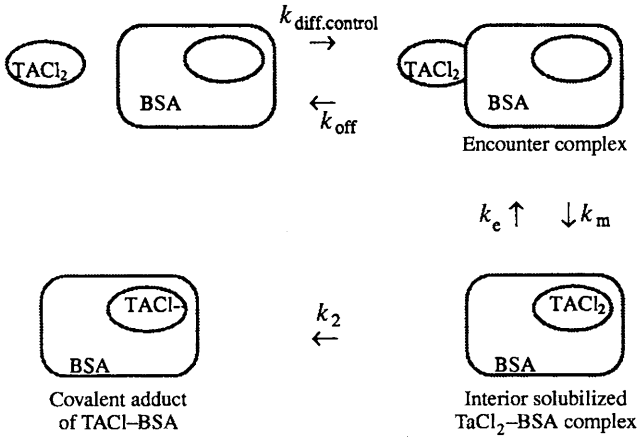

For each data set the rate constant k_{CP} can be found from the final limiting gradient of the $\ln(A_t/A_0)$ *versus* time plot, *i.e.*, in the later phase of the reaction. Scaling the time at which $\ln(A_t/A_0)$ attains -1.0 to $(k_{CP})^{-1}$ gives $z[-1]$, from which x can be obtained and thence k_{TC}. This approach relates to an analysis given by Jackson *et al.*[51] Hence, on the basis of our chosen model for data analysis, rate constant k_{CP} is equated to k_F, and rate constant k_{TC} is equated to k_I.

The rate constants evaluated in this way are collated in Table 10 for the reaction of BSA (2 mg cm^{-3} concentration in Tris–KCl buffer at pH 8.0) with $TACl_2$ (*ca.* 15 μmol dm^{-3} initial concentration) over the temperature range 293–323 K.

***(d)* Proposed scheme for the labelling reaction and its kinetics.** A simple physicochemical model is shown in Scheme 1. For clarity only one molecule of $TACl_2$ and one solubilizing pocket in the protein are considered. The encounter complex can be envisaged as association of the dye on the peripheral surface of the protein before migration and internalization of the dye molecule. Such a model has been elaborated for the kinetics of anti-thrombin inhibition of thrombin.[52–55]

Several kinetic situations can be envisaged, which can be compared with the empirical findings. If the forward and reverse reactions of the diffusional encounter and interior solubilization equilibria are rapid with respect to the chemical coupling step (governed by the rate constant k_p), then the system reduces kinetically to the form A ⟶ B. This entails strict first-order decay of the dye for the whole time course with the rate constant nearly linearly dependent on the protein concentration when the pre-equilibria lie towards free dye, but independent of the protein concentration when the equilibria are forced towards total complexation of the dye ligand. Here, this approximation model does not satisfy all the observed kinetic behaviour, for which two rate-limiting stages seem to be required.

From a Smoluchowski treatment of diffusional encounters of spherical particles having a mean radius R and diffusion coefficient D, the rate constants $k_{diff} = 8\pi LRD$ and $k_{off} = 6D/R^2$, and hence the equilibrium constant k_{EC}, can be estimated to a good order of magnitude.[56,57] For $R = 1.6$ nm and $D = 1 \times 10^{-6}$ cm^2 s^{-1}, $k_{diff} = 2.4 \times 10^9$ dm^3 mol^{-1} s^{-1}, $k_{off} = 2.3 \times 10^8$ s^{-1}, and the equilibrium constant $k_{EC} \approx 10$ dm^3 mol^{-1}. It is clear that the concentration of the encounter complex ≪ total concentration of dye at all relevant concentrations of the protein.

If it is assumed that the migration step, rate constant k_m, is a controlling factor and that the reverse (exit) step can be ignored relative to the adduct/product forming step, rate constant k_p, then kinetically k_{TC} (of the analysis scheme) equates to the composite term $k_m K_{EC}$ [BSA]$_0$. Since at short reaction times k_{TC} approximates closely to the initial gradient k_I of the experimental $\ln(A_t/A_0)$ *versus* time plot, the data given in Table 8 confirm this expected linear dependence of k_{TC} on the concentration of BSA protein. The rate constant k_m for the migration of unchanged dye from the periphery of the protein to its interior hydrophobic pocket can be estimated on this basis. At 298 K, k_{TC} is 1.10×10^{-2} s^{-1} for [BSA] = 30 μmol dm^{-3} and using $K_{EC} \approx 10$ dm^3 mol^{-1} yields $k_m = 37$ s^{-1}. The rate constant k_F can be equated to rate constant k_2 of the proposed reaction model (Scheme 1). From Arrhenius plots of $\ln k_I$ and of $\ln k_F$ *versus* reciprocal temperature, the activation energies of the T ⟶ C and C ⟶ P processes were calculated to be 65 ± 5 and 36 ± 3 kJ mol^{-1}, respectively. By comparison, the values for the calmodulin–$TACl_2$ reaction are similar, namely 77 and 21 kJ mol^{-1}, respectively.

As in the case of calmodulin the activation energy E_a (C ⟶ P) for the chemical coupling of the dye $TACl_2$ to a lysine ε-amino group inside a hydrophobic cavity of the protein BSA is significantly lower than that of the corresponding reaction in homogeneous media (50% v/v aqueous acetonitrile). The lowered activation enthalpy $\Delta H^{\ddagger}$ [$= E_a$(C ⟶ P) $- RT$] could arise from a partial prior removal of water from the inner solvation shell of the hydrophobic dye molecule, or may be a consequence of the microenvironmental shielding from water of the reactive lysine residue which enhances its ability to interact with the electrophilic carbon atom(s) of the triazinylaniline dye. However, from the pH dependence of the BSA–$TACl_2$ reaction (apparent $pK_a = 9.6$) the reactive residue is of lower basicity than free lysine in solution ($pK_a = 10.5$) and thus the former explanation may be preferred. From the data at 298.4 K and assuming a frequency factor of 10^{12} dm^3 mol^{-1} s^{-1} in the transition state theory expression, an entropy of activation of -71.5 J mol^{-1} K^{-1} is obtained, indicative of a strong immobilization of the dye and surrounding protein matrix in the chemical coupling step.

The activation energy E_a (T ⟶ C) for the combined diffusive encounter/solubilization steps is appreciable. Since the formation and dissolution of the initial encounter complex are most likely to possess low barriers (<20 kJ mol^{-1}) the major part (>50 kJ mol^{-1}) of E_a (T ⟶ C) must be attributed to energy barriers to internalization of the dye in the protein,[58] composed of conformational barriers to protein distortion/partial unfolding and also of partial desolvation of the entering dye molecule. Caution is advisable, however, in that dissection of the composite rate constant k_{TC} in an Arrhenius analysis may involve large errors.

In the case of $TACl_2$ the intrinsic rate constant for chemical coupling k_2 is slower than the effective rate constant for solubilization, such that the latter does not constitute a limiting factor. This situation might be reversed, however, for other more reactive dyes in protein labelling experiments but could be overcome by elevation of temperature.

Conclusions

The triazinylaniline dye *N*,*N*-diethyl-4-(dichloro-1,3,5-triazinyl)aniline shows the expected reactivities towards primary and secondary amines and amino acids. Control of reaction with amino acids, *e.g.*, *N*-terminal amino *versus* ε-amino group of a lysine side-chain, is best achieved by pH control of the concentration of the unprotonated active form of the

desired amino group. The relatively small differences in Arrhenius activation energies allow only a minor control of reaction pathway by adjustment of temperature.

Hydrophobic interactions of protein surfaces and dye reagent are crucial in determining both dye solubilization in the protein interior and high selectivity of reaction coupling to specific residues. Initial rapid diffusional encounter of dye and protein is followed by a slower 'internalization' of the dye having an appreciable energy barrier (≈70 kJ mol^{-1}). Chemical adduct formation then follows with, in general, a reactive lysine residue sterically accessible to the dye, which is constrained by hydrophobic and hydrogen bonding interactions to the 'inner' surface of the protein.

References

1 D. J. Cowley, E. O'Kane and R. S. J. Todd, *J. Chem. Soc., Perkin Trans. 2*, 1991, 1495.
2 D. J. Cowley and R. S. J. Todd, *J. Chem. Soc., Perkin Trans. 2*, 1995, 299.
3 D. J. Cowley and J. P. McCormick, *J. Chem. Soc., Perkin Trans. 2*, 1996, 1677.
4 R. F. Steiner and H. Edelhoch, *Chem. Rev.*, 1962, **62**, 457.
5 L. Stryer, *Annu. Rev. Biochem.*, 1985, **54**, 43.
6 (*a*) R. P. Haugland, *Handbook of Fluorescent Probes and Research Chemicals*, 6th edn., Molecular Probes, Eugene, USA, 1994; (*b*) R. P. Haugland in *Excited States of Biopolymers*, ed. R. F. Steiner, Plenum Press, London, 1983, ch. 2, and references therein.
7 K. Torok, A. N. Lane, S. R. Martin, J.-M. Janot and P. M. Bayley, *Biochemistry*, 1992, **31**, 5269.
8 V. Saudek and J. T. Pelton, *Biochemistry*, 1990, **29**, 4509.
9 R. A. Shaw and P. Ward, *J. Chem. Soc. B*, 1967, 123.
10 R. A. Shaw and P. Ward, *J. Chem. Soc., Perkin Trans. 2*, 1973, 2075.
11 E. M. Smolin and L. Rapoport in *The Chemistry of Heterocyclic Compounds*, Vol. 13, *s-Triazines and their Derivatives*, Interscience, New York, 1959.
12 R. G. Shepherd and J. L. Frederick, *Adv. Heterocycl. Chem.*, 1965, **4**, 145.
13 F. Pietra, *Quart. Rev. (London)*, 1969, **23**, 504.
14 M. R. Crampton and P. J. Routledge, *J. Chem. Soc., Perkin Trans. 2*, 1984, 573.
15 C. F. Bernasconi and R. H. de Rossi, *J. Org. Chem.*, 1976, **41**, 44.
16 J. F. Bunnett and A. V. Cartano, *J. Am. Chem. Soc.*, 1981, **103**, 4861.
17 C. F. Bernasconi, *Acc. Chem. Res.*, 1978, **11**, 147.
18 P. Rys, A. Schmitz and H. Zollinger, *Helv. Chim. Acta*, 1971, **54**, 163.
19 G. Illuminati, *Adv. Heterocycl. Chem.*, 1964, **3**, 285.
20 R. P. Oomen and H. Kaplan, *Biochemistry*, 1992, **31**, 5698.
21 P. A. Alred, G. Johansson and F. Tjerneld, *Anal. Biochem.*, 1992, **205**, 351.
22 P. Tsitsa, E. Antoniadou-Vyza, S. J. Hamodrakas, E. E. Eliopoulos, A. Tsanttili-Kakoulidou, E. lada-Hytiroglou, C. Roussakis, I. Chinou, A. Hempel, N. Cameran, F. P. Ottensmayer and D. A. Vanden Berghe, *Eur. J. Med. Chem.*, 1993, **28**, 149.
23 U. Egner, G.-A. Hoyer and W. Saenger, *Eur. J. Biochem.*, 1992, **206**, 685.
24 D. Bashford and M. Karplus, *Biochemistry*, 1990, **29**, 10219.
25 K. Torok, D. J. Cowley, B. D. Brandmeier, S. Howell, A. Aitkin and D. R. Trentham, *Biochemistry*, in the press.
26 K. Torok and D. R. Trentham, *Biochemistry*, 1994, **33**, 12807.
27 A. Persechini and R. H. Kretsinger, *J. Biol. Chem.*, 1988, **263**, 12175.
28 R. H. Kretsinger, *Cell Calcium*, 1992, **13**, 363.
29 J. Mackall and C. B. Klee, *Biochemistry*, 1991, **30**, 7242.
30 C. B. Klee in *Calmodulin*, vol. 5, eds. P. Cohen and C. B. Klee, Elsevier, Amsterdam, 1988, pp. 35–56.
31 H. Kuboniwa, N. Tjandra, S. Grzesiek, H. Ren, C. B. Klee and A. Bax, *Nature, Struct. Biol.*, 1995, **2**, 768.
32 B. E. Finn, J. Evenas, T. Drakenberg, J. P. Waltho, E. Thulin and S. Forsen, *Nature. Struct. Biol.*, 1995, **2**, 777.
33 W. E. Meador, S. E. George, A. R. Means and F. A. Quiocho, *Nature Struct. Biol.*, 1995, **2**, 943.
34 B. E. Finn and S. Forsen, *Structure*, 1995, **3**, 7.
35 M. Milos, M. Comte, J. J. Schaer and J. A. Cox, *J. Inorg. Biochem.*, 1989, **36**, 11.
36 D. Lafitte, J. P. Capony, G. Grassy, J. Haiech and B. Calas, *Biochemistry*, 1995, **34**, 13825.
37 S. R. Martin, A. Andersson Teleman, P. M. Bayley, T. Drakenberg and S. Forsen, *Eur. J. Biochem.*, 1985, **151**, 543.
38 D. P. Giedroc, D. Puett, S. K. Sinha and K. Brew, *Arch. Biochem. Biophys.*, 1987, **252**, 136.
39 Q. Wei, A. E. Jackson, S. Pervaiz, K. L. Carraway III, E. Y. C. Lee, D. Puett and K. Brew, *J. Biol. Chem.*, 1988, **263**, 19541.
40 L. D. Dwyer, P. J. Cocker, D. S. Watt and T. C. Vanaman, *J. Biol. Chem.*, 1992, **267**, 22606.
41 D. M. Mann and T. C. Vanaman, *J. Biol. Chem.*, 1988, **263**, 11284.
42 F. M. Faust, M. Slisz and H. W. Jarrett, *J. Biol. Chem.*, 1987, **262**, 1938.
43 B. B. Olwin and D. R. Storm in *Methods in Enzymology*, vol. 102, Academic Press, New York, 1983, pp. 148–157.
44 J. R. Brown and P. Schockley in *Lipid–Protein Interactions*, eds. P. C. Jost and O. H. Griffin, Wiley, New York, 1982, vol. 1, pp. 1–26.
45 D. C. Wilton, *Biochem. J.*, 1990, **270**, 163.
46 S. Cohen and R. Margalit, *Biochem. J.*, 1990, **270**, 325.
47 M. L. Fonda, C. Trauss and U. M. Guempel, *Arch. Biochem. Biophys.*, 1991, **288**, 79.
48 U. Kragh-Hansen, *Biochem. J.*, 1991, **273**, 6419.
49 K. Hirayama, S. Akashi, M. Furuya and K. Fukuhara, *Biochem. Biophys. Res. Commun.*, 1990, **173**, 639.
50 J. W. Moore and R. G. Pearson, *Kinetics and Mechanism*, 3rd edn., Wiley, New York, 1981.
51 W. G. Jackson, J. M. Harrowfield and P. D. Vowles, *Int. J. Chem. Kinet.*, 1977, **9**, 535.
52 J. F. Morrison and C. T. Walsh, *Adv. Enzymol. Relat. Areas Mol. Biol.*, 1988, **61**, 201.
53 A. R. Rezaie, *Biochemistry*, 1996, **35**. 1918.
54 S. T. Olsen and J. D. Shore, *J. Biol. Chem.*, 1982, **257**, 14891.
55 S. R. Stone and J. M. Hermans, *Biochemistry*, 1995, **34**, 5164.
56 J. Lansman and D. H. Hayes, *Biochim. Biophys. Acta*, 1975, **394**, 335.
57 P. D. Lampe, G. J. Wei and G. L. Nelsestuen, *Biochemistry*, 1983, **22**, 1594.
58 E. T. Rakitzis, *Biochem. J.*, 1990, **269**, 835.

Paper 6/02443B
Received 9*th April* 1996
Accepted 30*th May* 1996